JOURNAL OF BONE AND MINERAL RESEARCH
Volume 23, Number 5, 2008
Published online on February 4, 2008; doi: 10.1359/JBMR.080204

Mutations in the Insulin-Like Factor 3 Receptor Are Associated With Osteoporosis

Alberto Ferlin,[1] Anastasia Pepe,[1] Lisa Gianesello,[1] Andrea Garolla,[1] Shu Feng,[2] Sandro Giannini,[3] Manuela Zaccolo,[4,5] Arianna Facciolli,[1] Roy Morello,[6] Alexander I Agoulnik,[2] and Carlo Foresta[1]

ABSTRACT:

Introduction: Insulin-like factor 3 (INSL3) is produced primarily by testicular Leydig cells. It acts by binding to its specific G protein–coupled receptor RXFP2 (relaxin family peptide 2) and is involved in testicular descent during fetal development. The physiological role of INSL3 in adults is not known, although substantial INSL3 circulating levels are present. The aim of this study was to verify whether reduced INSL3 activity could cause or contribute to some signs of hypogonadism, such as reduced BMD, currently attributed to testosterone deficiency.
Materials and Methods: Extensive clinical, biochemical, and hormonal study, including bone densitometry by DXA, was performed on 25 young men (age, 27–41 yr) with the well-characterized T222P mutation in the *RXFP2* gene. Expression analysis of INSL3 and RXFP2 on human bone biopsy and human and mouse osteoblast cell cultures was performed by RT-PCR, quantitative RT-PCR, and immunohistochemistry. Real-time cAMP imaging analysis and proliferation assay under the stimulus of INSL3 was performed on these cells. Lumbar spine and femoral bone of *Rxfp2*-deficient mice were studied by static and dynamic histomorphometry and μCT, respectively.
Results: Sixteen of 25 (64%) young men with *RXFP2* mutations had significantly reduced BMD. No other apparent cause of osteoporosis was evident in these subjects, whose testosterone levels and gonadal function were normal. Expression analyses showed the presence of RXFP2 in human and mouse osteoblasts. Stimulation of these cells with INSL3 produced a dose- and time-dependent increase in cAMP and cell proliferation, confirming the functionality of the RXFP2/INSL3 receptor–ligand complex. Consistent with the human phenotype, bone histomorphometric and μCT analyses of $Rxfp2^{-/-}$ mice showed decreased bone mass, mineralizing surface, bone formation, and osteoclast surface compared with wildtype littermates.
Conclusions: This study suggests for the first time a role for INSL3/RXFP2 signaling in bone metabolism and links *RXFP2* gene mutations with human osteoporosis.
J Bone Miner Res 2008;23:683–693. Published online on February 4, 2008; doi: 10.1359/JBMR.080204

Key words: osteoporosis, insulin-like factor 3, relaxin family peptide, hypogonadism, leucine-rich repeat–containing G protein–coupled receptor 8

INTRODUCTION

INSULIN-LIKE FACTOR 3 (INSL3)[1] is a member of the relaxin-like peptide family, and it is emerging as a key factor in the regulation of a variety of developmental processes related to reproduction.[2,3] The binding of the hormone to its specific receptor RXFP2 (also known as leucine-rich repeat–containing G protein–coupled receptor 8 [LGR8])[4–7] activates adenylate cyclase and cAMP production through Gs proteins, although alternative mechanisms have been proposed.[8,9]

INSL3 is expressed in pre- and postnatal Leydig cells of the testis. The major known endocrine role of INSL3 is related to the regulation of the transabdominal phase of testicular descent by action on the gubernaculum.[4,10–12] As a consequence, *Insl3* and *Rxfp2* knockout mice have bilateral cryptorchid testes,[4,10–12] and mutations in the *INSL3* and *RXFP2* genes have been associated with testis maldescent also in humans.[10,13–15]

In addition to the prenatal role for INSL3, further possible endocrine and paracrine actions in adult males have recently gained particular attention based on several observations. First, in adults, INSL3 is produced constitutively

The authors state that they have no conflicts of interest.

[1]Department of Histology, Microbiology and Medical Biotechnologies, Section of Clinical Pathology and Centre for Male Gamete Cryopreservation, University of Padova, Padova, Italy; [2]Department of Obstetrics and Gynecology, Baylor College of Medicine, Houston, Texas, USA; [3]Department of Medical and Surgical Sciences, Clinica Medica 1, University of Padova, Padova, Italy; [4]Dulbecco Telethon Institute, Venetian Institute of Molecular Medicine, Padova, Italy; [5]Division of Biochemistry and Molecular Biology, IBLS, University of Glasgow, Glasgow, Scotland; [6]Department of Molecular and Human Genetics, Baylor College of Medicine, Houston, Texas, USA.

but in a differentiation-dependent manner by the Leydig cells under the long-term Leydig cell differentiation effect of luteinizing hormone (LH), and substantial circulating INSL3 levels are present in adult men.[2,16,17] Reduced plasma concentrations are seen in situations of undifferentiated or altered Leydig cell status (such as hypogonadism), and INSL3 has been suggested to be even more sensitive than testosterone to impaired Leydig cell function.[2,16,18] Second, RXFP2 is expressed in many tissues besides the gubernaculum, including kidney, skeletal muscle, thyroid, pituitary gland, brain, and bone marrow,[2,4,5] and paracrine roles for INSL3 have been suggested in the testis,[19,20] ovary,[19] thyroid,[21] and mammary gland.[22]

With this scenario, our hypothesis was that reduced INSL3 activity (caused by altered testicular function, *INSL3* or *RXFP2* gene mutations) could cause or contribute to some symptoms and signs of hypogonadism, such as reduced BMD, currently attributed to testosterone deficiency. To clarify potential endocrine roles of INSL3 in adults, we recruited 25 adult young men (age, 27–41 yr) with the T222P mutation in the *RXFP2* gene. We selected men with this mutation because previous analysis showed that INSL3/RXFP2-mediated cAMP production in cells transfected with a T222P mutant receptor is strongly decreased because of a reduction of receptor surface expression that renders the protein functionally inactive.[6,15]

MATERIALS AND METHODS

Subjects

We enrolled 25 young men (age, 27–41 yr) with the T222P mutation in the *RXFP2* gene identified among subjects screened for cryptorchidism. Seventeen men reported unilateral and eight reported bilateral cryptorchidism at birth and were orchidopexied at 1–8 yr of age. All men were of white origin (Italian) and had a normal 46,XY karyotype; mutations in *INSL3* and androgen receptor genes were excluded.[14] T222P mutation was evaluated on genomic DNA extracted from peripheral blood by denaturing high-performance liquid chromatography (DHPLC) and direct sequencing as previously reported.[10,14] Informed consent was obtained from each subject; the study conformed to the standards set by the Declaration of Helsinki and was approved by the University of Padova Institutional Review Board. Clinical study included a careful history and physical examination. Measurement of bone densitometry was done by DXA in the femoral neck and lumbar spine (L_1–L_4), and T-score was calculated (the number of SDs the BMD measurement is above or below the young-normal mean BMD). No subjects had chronic or skeletal disorders, malnutrition, or uro-andrological abnormalities, and none used drugs affecting bone metabolism. All of them had normal body mass index (Table 1), normal hemogram, erythrocyte sedimentation rate, biochemical parameters (serum glucose, lipids, transaminases, urea, uric acid, creatinine, osteocalcin, calcium, phosphorus, alkaline phosphatase), and urine analysis (including creatinine, hydroxyproline, deoxypyridinoline, calcium, and phosphorus excretion). Furthermore, testosterone, sex hormone–binding globulin (SHBG), LH, follicle-stimulating hormone (FSH), prolactin (PRL), estradiol, INSL3, progesterone, cortisol, thyroid hormones (FT3 and FT4), thyroid-stimulating hormone (TSH), growth hormone (GH), insulin-like growth factor I (IGF-I), PTH, vitamin D, and calcitonin concentrations were measured and in the normal range. Free testosterone was calculated from total T and SHBG concentrations using the method of Vermeulen et al.[23] and was normal in all cases. All subjects had normal food intake (in particular for calcium) and had normal physical activity. The timing of puberty was normal and spontaneous in all patients. Fifty-one healthy Italian subjects (age, 30–45 yr) and 20 men with surgically corrected cryptorchidism without *RXFP2* and *INSL3* mutations (age, 25–40 yr) were included as controls for DXA analysis.

Cell cultures and transfections

The human osteoblast cell line MG-63 (ICLC, Genova, Italy) was propagated in DMEM/F-12 (Invitrogen, Milan, Italy) supplemented with 10% FBS (Celbio, Milan, Italy), 1 mM glutamine (Invitrogen), and an antibiotic mixture of penicillin (100 U/ml) and streptomycin (100 μg/ml; Sigma-Aldrich, Milan, Italy). 293T cells derived from human embryonic kidney (HEK) fibroblasts (ICLC) were maintained in DMEM (Invitrogen) supplemented with 10% FBS and the antibiotic mixture previously described. Human male primary osteoblast cells (Dominion Pharmakine, Derio, Spain) were cultured in DMEM/F-12 Ham (Invitrogen), 10% FBS, penicillin (100 U/ml), and streptomycin (100 μg/ml). The HIT-T15 cell line (ATCC, Manassas, VA, USA) was subcultured in RPMI 1640 medium (Invitrogen) supplemented with 2.5% FBS, 10% horse serum (Celbio), and the antibiotic mixture penicillin/streptomycin as described above. One day before transfection, HIT-T15 and 293T cells were seeded into 25-cm^2 cell culture flasks at high density to achieve 60–80% confluency. All cell lines were grown in a 5% CO_2 atmosphere at 37°C. *RXFP2* cDNA expression construct (*LGR8*-FLAG in pCR3.1)[15] and *INSL3* cDNA expression construct (*INSL3* in pcDNA3.1 myc/His B)[7] were used to transfect 293T and HIT-T15 cells, respectively. Plasmids were purified with the QIAfilter Plasmid Midi kit (Qiagen, Milan, Italy). 293T and HIT-T15 cells were transfected at 70% and 60%, respectively, of confluency using the FuGENE 6 Transfection Reagent (Roche, Mannheim, Germany) following the manufacturer's instructions with the following amounts of DNA: for T-25 293T cells, 1.6 μg of plasmid pCR 3.1 with RXFP2 expression construct; for T-25 HIT-T15 cells, 5 μg of the expression construct encoding INSL3 peptide in Opti-MEM (Invitrogen) without serum and antibiotics.

Primary osteoblasts were released from P4 mouse calvariae by digestion with 0.1 mg/ml Collagenase P (Roche Molecular Biochemicals) and 0.04% Tripsin/EDTA in serum-free medium for 1 h at 37°C and grown in α-MEM, 10% FBS, 2 mM glutamine, penicillin (100 U/ml), and streptomycin (100 μg/ml). After 2 days in culture, they were trypsinized, replated at a 1–1.5 × 10^4 cells/cm^2 density, and grown in mineralization medium containing 5 mM β-glycerophosphate and 100 μg/ml ascorbic acid.

TABLE 1. RESULTS OF BONE DENSITOMETRY BY DXA IN 25 SUBJECTS WITH THE T222P MUTATION IN THE *RXFP2* GENE

Patient no.	*Age (yr)*	*Weight (kg)*	*Height (cm)*	*Testosterone (nM)*	*SHBG (nM)*	*Free T (pM)*	*LH (IU/liter)*	*FSH (IU/liter)*	*Estradiol (pM)*	*INSL3 (pg/ml)*	*DXA femoral neck T-score SD*	*DXA lumbar spine L_1–L_4 T-score SD*	*Classification*
2445	41	58	169	19.2	39	372	3.7	5.1	78	458	–2.0	–0.8	Osteopenia
2463	31	67	170	14.4	22	365	5.4	1.8	71	622	–1.8	–2.2	Osteopenia
2479	41	75	175	26.2	30	630	4.5	4.7	87	780	–2.4	–2.8	Osteoporosis
2552	32	75	183	16.9	19	466	3.3	1.6	62	542	0.7	0.4	Normal
2564	29	72	175	14.7	24	359	1.7	2.5	34	800	1.1	0.7	Normal
2577	40	79	178	21.2	42	399	2.5	2.9	55	424	–0.2	–0.7	Normal
2642	32	72	176	15.6	16	455	5.5	6.2	96	340	1.7	1.9	Normal
2654	33	57	169	18.9	23	488	6.1	3.9	79	826	–0.5	0.4	Normal
2742	33	68	172	19.8	18	569	2.2	2.4	30	870	–1.3	–0.9	Osteopenia
2761	34	74	175	17.2	29	390	3.9	1.1	20	612	–1.8	–0.3	Osteopenia
2804	35	71	174	22.5	35	480	1.6	1.7	124	550	–2.9	–2.2	Osteoporosis
2821	36	80	180	16.8	50	268	2.2	1.0	44	448	–1.6	–2.1	Osteopenia
2864	35	63	167	14.6	10	485	5.1	3.7	110	328	–0.5	0.6	Normal
2907	28	85	185	12.0	22	298	4.0	5.7	74	772	–1.1	–1.4	Osteopenia
3007	35	71	174	20.2	34	430	2.4	2.3	102	780	–0.7	–1.0	Normal
3013	27	80	183	20.0	30	456	1.7	1.4	50	910	–1.6	–2.6	Osteoporosis
3429	38	78	180	19.4	24	493	2.0	3.4	25	656	–2.0	–2.6	Osteoporosis
3587	32	70	171	25.2	22	695	3.2	6.4	92	640	–1.8	–2.8	Osteoporosis
3743	36	69	168	19.7	34	417	1.8	4.0	14	726	–0.5	–0.5	Normal
3834	31	78	178	22.0	14	697	2.6	3.5	66	660	–1.5	–1.4	Osteopenia
4011	33	72	172	21.0	40	407	4.9	5.5	42	520	–2.6	–2.8	Osteoporosis
4352	30	63	173	18.6	34	390	3.1	2.6	18	580	–1.4	–1.8	Osteopenia
4365	40	68	178	17.8	55	268	2.9	4.4	36	724	–1.4	–0.7	Osteopenia
4419	35	54	164	22.0	46	392	4.0	5.1	100	1012	–1.0	–1.3	Osteopenia
4550	36	78	178	18.0	43	323	2.0	1.8	26	544	–0.2	–0.5	Normal
Mean ± SD	34.1 ± 3.9	71.1 ± 7.7	174.7 ± 5.3	19.0 ± 3.3	30.2 ± 11.7	439.7 ± 114.4	3.2 ± 1.3	3.4 ± 1.7	61.4 ± 32.1	645.0 ± 176.2	–1.1 ± 1.1	–1.1 ± 1.3	

Osteopenia is defined as a T-score < –1 SD and osteoporosis as a T-score < –2.5 SD of the young-normal mean BMD. Reference ranges for reproductive hormones are as follows: testosterone, 10–29 nM; SHBG, 10–70 nM; free testosterone, 250–900 pM; LH, 1–9 UI/liter; FSH, 1–8 IU/liter; estradiol, 25–130 pM; INSL3, 300–900 pg/ml.

TABLE 2. OLIGONUCLEOTIDE PRIMERS USED IN PCR REACTIONS WITH POSITIONS, ANNEALING TEMPERATURES, AND FRAGMENT SIZES

Name	*Sequence*	*Exon*	*Annealing temperature*	*Size (bp)*
Human				
β-actin forward	5′-CACTCTTCCAGCCTTCCTTCC-3′	3	58°C	318
β-actin reverse	5′-CGGACTCGTCATACTCCTGCTT-3′	5		
RXFP2 3′UTR forward	5′-TGCACAGAGAGCACAGCAGAATGGCTC-3′	3′ UTR	65°C	241
RXFP2 3′UTR reverse	5′-GGACAGTGCAACCCGATGTGAAAGACC-3′	3′ UTR		
RXFP2 F2	5′-CTCAACTCATATAGCTCTTG-3′	17	58°C	332
RXFP2 R2	5′-CTACAGAACACCAAATCAGC-3′	18		
RXFP2 96 forward	5′-GTATGCCCTTGACGGACGG-3′	15	60°C	338
RXFP2 97 reverse	5′-CAGAACAGAGACTTCGGTGG-3′	16		
RXFP2 5F	5′-GATCACTCCTTCATGCCAAAAA-3′	2	55°C	139
RXFP2 m-hR	5′-CCATCCACTAGTGTCACCACA-3′	2–3		
INSL3 forward	5′-GCGTGAGAAGTTGTGCGGC-3′	1	64°C	269
INSL3 reverse	5′-CACTGAGGCAGCAGTAGCG-3′	2		
RXFP1 forward	5′-GAGATGATCCTTGCCAAACG-3′	17	58°C	294
RXFP1 reverse	5′-CACCCAGATGAATGATGGAG-3′	18		
Mouse				
Rxfp2 1exF	5′-CGAACTCAATGCTGCAAATC-3′	1	55°C	278
RXFP2 m-hR	5′-CCATCCACTAGTGTCACCACA-3′	2–3		
Insl3 F	5′-TACTGATGCTCCTGGCTCTG-3′	1	55°C	199
Insl3 R	5′-TGCAGGAGATGTCTCTGCTCT-3′	2		

RNA isolation and cDNA synthesis

Total RNA from human osteoblast cells was isolated with RNA-Bee reagent (TEL-TEST, Friendswood, TX, USA). The amount of RNA isolated was determined by spectrometry at 260 and 280 nm. Total RNA (<50 ng) obtained from the osteoblast cell lines was used for first-strand cDNA synthesis using the Sensiscript Reverse Transcriptase kit (Qiagen) according to the manufacturer's instructions: 1× buffer RT, 0.5 mM each dNTP, 10 μM random hexamer primers (Invitrogen), 10 U RNase inhibitor, and 1 μl Sensiscript Reverse Transcriptase in a final volume of 20 μl. Products of RT reactions (cDNAs) were tested by PCR using specific oligonucleotide primers for the housekeeping gene *β-actin* (Table 2). The Marathon cDNA pool from human testis library (BD Clontech, Palo Alto, CA, USA) was used as a control. Vertebral bone biopsies were obtained during orthopedic surgical procedures from juvenile male scoliotic patients with written consent. Small bone fragments were cleaned of any muscle residues, frozen in liquid nitrogen, crushed with a pestle, and further homogenized into Trizol Reagent (Invitrogen). Total RNA was obtained following Trizol manufacturer recommendations.

RNA from mouse primary calvarial osteoblasts was prepared either after 2 or 10 days of culture in mineralizing medium using Trizol Reagent (Invitrogen). Total human and mouse RNA (1 μg) was used to synthesize cDNA with the Superscript III First-Strand kit (Invitrogen) according to the manufacturer's instructions. Testis cDNA was prepared from adult male mice as a positive control for amplification of the mouse genes.

Expression of RXFP2 and INSL3: PCR and quantitative PCR

PCRs were performed on cDNA obtained from osteoblast cells. For the amplification of the coding sequence of human *INSL3* and the amplification of the partial coding sequence of *RXFP2*, specific intron spanning oligonucleotide primers (Table 2) were used to preclude any genomic DNA amplification. PCR reactions were carried out in a final volume of 25 μl containing 5 μl of cDNA, 1× *Taq* Gold Buffer, 1.5 mM $MgCl_2$, 100 μM each dNTP, 100 ng each primer, and 1 U *Taq* Gold DNA-polymerase (Roche, Mannheim, Germany). The PCR cycles consisted of an initial denaturation for 10 min at 95°C, annealing for 45 s, and elongation for 1 min at 72°C, all followed by 40 cycles of denaturation at 95°C for 45 s, annealing for 45 s, and elongation at 72°C for 1 min and a final extension cycle at 72°C for 10 min. The annealing temperature was optimized for each fragment (Table 2), and reactions were performed in a PTC-100 Thermal cycler (MJ Research). Amplification products were confirmed by direct sequencing. Negative controls were performed by using water instead of cDNA.

Quantitative expression of RXFP2 in human primary osteoblasts was evaluated with respect to testis and PTH receptor 1 (PTHR1). Oligonucleotides for PTHR1 and RXFP2 were chosen from predesigned assays (TaqMan Gene Expression Assays; Applied Biosystems; Hs00174895_ml and Hs00373113_ml, respectively). Thermal cycling included initial steps at 50°C for 2 min and at 95°C for 10 min, followed by 40 cycles at 95°C for 15 s and at 60°C for 1 min. The fluorescence of the double-stranded products was monitored in real time. The cDNA was amplified and quantified using a Sequence Detection System SDS 7900 (Applied Biosystems). Data were normalized to an internal housekeeping gene, using TaqMan Human β-actin (ACTB) MGB (Applied Biosystems). Experiments were performed three times in triplicate. Data elaboration was performed as relative quantification analysis using the ΔΔCt method.

Expression of RXFP2: Western blot analysis

Western blot detection of RXFP2 in protein extracts of osteoblast cell lines MG-63 and 293T cells transfected and not (vector; harvested 24 h after transfection) was performed with a polyclonal rabbit antibody generated against the 18-mer sequence located at the C-terminal end of the receptor ($^{N'}$LGVLNKITLGDSIMKPVS$^{C'}$; Phoenix Pharmaceutical, Belmont, CA, USA). Commercial protein extracts of testis, prostate, and adrenal gland (BD Clontech, Palo Alto, CA, USA) were used as controls. Cell line lysates were obtained by a physical procedure (freezing in liquid nitrogen and defrosting in water at 37°C). Lysates were denatured with SDS and 2-β-mercaptoethanol and fractionated using SDS-PAGE. After blotting onto Hybond ECL Nitrocellulose Membrane (Amersham Biosciences, Uppsala, Sweden) and blocking with a 0.1% milk solution (Bio-Rad, Milan, Italy), blots were incubated at 4°C with the anti-LGR8 antibody diluted 1:1500 overnight. After washing with TBS-T (3 × 10 min), specific binding was detected with a peroxidase-conjugated donkey anti-rabbit immunoglobulin (Amersham Biosciences) diluted 1: 20,000 in TBS-T and revealed with the enhanced chemiluminescence ECL reagent (Amersham Biosciences).

Expression of RXFP2 and INSL3: immunohistochemistry

MG-63 cells and the primary osteoblast cells were immunostained using the Vectastain ABC Elite Kit (Vector Laboratories, Burlingame, CA, USA) with the polyclonal anti-RXFP2 used for Western blot analysis and with a purified IgG antibody against human INSL3 (Phoenix Pharmaceutical, Belmont, CA, USA). Cells were fixed in 4% formaldehyde at room temperature for 20 min and washed with PBS. Specimens were treated with PBS-Triton 3% for 10 min and with 3% H_2O_2 in PBS for 15 min, followed by blocking with 10% normal goat serum (NGS) for 30 min. Samples were incubated with primary antibody (anti-RXFP2, 1:2000; anti-INSL3, 1:1000) at 4°C overnight. After two quick rinses (the first one in PBS containing 0.01% Triton and the second one in PBS only), cells were incubated in biotinylated goat anti-rabbit immunoglobulin 1: 100–500 for 60 min. After washing again in PBS-Triton 0.01% and PBS, the reaction between primary and secondary antibody was amplified by incubating cells in ABC complex for 45 min at room temperature and staining with diaminobenzidine tetrahydrochloride (DAB) until optimal staining. Cells were counterstained with hematoxylin and were processed for visualization of RXFP2 and INSL3. Specimens were examined with an inverted microscope. Negative controls were performed by omitting the primary antibody.

Functionality of RXFP2: fluorescence resonance energy transfer imaging

293T cells and MG63 osteoblast cells were seeded on round glass coverslips, cultured, and transfected with fluorescence resonance energy transfer (FRET) probe for cAMP. This sensor is formed by a ΔDEP, catalytically dead Epac protein sandwiched between cyan fluorescence protein (CFP) and yellow-fluorescence protein (YFP).[24,25] 293T cells were co-transfected with the Epac-based sensor and RXFP2 constructs using Fugene6 Reagent. Transfection in osteoblast cell lines was made with Arrest-In Transfection Reagent (Open Biosystem; Celbio). Experiments were performed in a culture chamber in a saline buffer (NaCl 125 mM, KCl 5 mM, Na_3PO_4 1 mM, $MgSO_4$ 1 mM, HEPES 20 mM, Glucose 5.5 mM, $CaCl_2$ 1 mM). We used as agonists INSL3 and recombinant human relaxin H2 (both from Phoenix Pharmaceutical) in different concentrations (INSL3: 0.14, 1.4, and 10.4 nM; RLX-H2: 0.59 and 1.4 nM) diluted in the same buffer.

In each experiment, we first inhibited phosphodiesterase with IBMX (100 μM final), and at the end of the experiment, cell viability was assessed by overstimulating the adenylate cyclase with forskolin (25 μM final). When the Epac-based sensor has its binding sites for cAMP free, it has a conformation that enables FRET between CFP and YFP. When it binds cAMP, the Epac-based sensor changes its conformation, and the distance between CFP and YFP is no longer compatible with energy transfer by resonance. In the FRET imaging experiments, only CFP is directly excited at 430 nm, and emission intensities are collected both from CFP (480 nm) and YFP (545 nm). When cAMP binds the sensor, the efficiency of energy transfer decreases, and a drop in YFP emission is recorded. FRET monitoring was performed as described[26] using an inverted Olympus IX50 microscope, equipped with a cooled-CCD camera (Sensiscam QI; PCO), with a software controlled monochromator (TILL Photonics) and a beam splitter optical device (Microimager; Optical Insight). Images were acquired using custom-made software[24,26] and processed using ImageJ (WS Rasband, ImageJ; NIH, Bethesda, MD, USA). Exposure time was 200 ms, and images were acquired every 5 s and exited the sample at 425 nm. Data were digitalized, and FRET was expressed as a ratio of CFP to YFP signals that was normalized as percent deviation from the initial value set to 1.0 at the onset of the experiment. Each experiment was performed 5–10 times, and the representative experiments, reproducing the results of such repeats, are shown in figures.

Cell proliferation assay

Proliferation of human primary osteoblasts was measured by a colorimetric assay based on the cleavage of tetrazolium salts (WST-1; Roche Molecular Biochemicals) by mitochondrial dehydrogenase. Cells (2×10^4 cells/well) were plated onto 96-well plates and incubated with INSL3 at different concentrations (10^{-8}, 10^{-10}, and 10^{-11}M) for 72 h. WST-1 was added to each well according to the manufacturer's instructions and incubated for 4 h at 37 C and 5% CO_2. Finally, the absorbance at 440 nm was measured with an ELISA reader. Experiments were performed in triplicate and repeated three times. Data are expressed as percentages with respect to control.

Rxfp2-deficient mice

The heterozygous *Rxfp*$^{-/+}$ mice[10] (14th generation of backcrosses to FVB inbred strain) were mated to produce wildtype, heterozygous, and mutant homozygous progeny.

The genotype of the animals was determined by tail DNA analysis as previously described.[10] Eight-week-old males were used for analysis of bone histology. Testosterone levels of wildtype and cryptorchid mice were not different in the two groups (2.04 ± 0.80 and 2.08 ± 0.93 ng/ml, respectively). The weight of the WT and KO mice was 25.7 ± 0.8 and 27.6 ± 1.9 g, respectively. Serum testosterone levels were analyzed by radioimmunoassay (RIA) in the University of Virginia Center for Research in Reproduction Ligand Assay and Analysis Core. All experiments were conducted using the standards for humane care in accordance with NIH Guide for the Care and Use of Laboratory Animals and were approved by the Baylor College of Medicine Animal Care and Use Committee.

Bone analysis of mice

Histomorphometric analysis of static bone parameters was carried out according to standard procedures[27,28] in 8-wk-old *Rxfp2*$^{-/-}$ ($n = 7$) and *Rxfp2*$^{+/+}$ ($n = 7$, WT) male mouse lumbar spines. Briefly, the lumbar spine was collected, fixed in 10% buffered formalin for 48 h, dehydrated, and embedded in methylmethacrylate. Medial sections through the vertebral bodies of L_3 and L_4 were generated, and BV/TV and trabecular thickness values were calculated by averaging four measurements taken from L_3 and L_4 in two different von Kossa–stained 7-μm-thick sections 30–40 μm away from each other. The sections were analyzed using TAS software (trabecular analysis software), which is part of the Osteometrics image analysis system (Osteo-Metrics, Decatur, GA, USA). Serial 5-μm-thick sections of L_3–L_4 were also stained with toluidine blue and TRACP, according to standard protocols, for counting osteoblasts and osteoclasts, respectively. Osteoblasts and osteoclasts data were obtained counting at least 100 fields at ×40 magnification of the L_4 vertebral body using the Osteometrics software.

Dynamic parameters of bone formation (mineralizing surface [MS/BS], mineral apposition rate [MAR], bone formation rate [BFR]) were obtained in 8-wk-old *Rxfp2*$^{-/-}$ ($n = 4$) and WT ($n = 4$) male mouse lumbar spines; the mice were injected with alizarin-3-methylmino-diacetic acid (25 mg/kg) and 4 days later with calcein (25 mg/kg) and killed 2 days after the second injection. At least 28–30 fields at ×20 magnification of L_4 were analyzed with Osteometrics.

μCT analysis and 3D reconstruction of *Rxfp2*$^{-/-}$ and WT intact femurs ($n = 7$) were performed using a Scanco 40 instrument (Scanco Medical, Bassersdorf, Switzerland) at a slice resolution of 12 μm. The samples were scanned from the midshaft portion down to include the complete distal femur epiphysis, with an effective energy of 55 kVp and X-ray tube current of 145 μA, generating ~700 slices. For the quantification of cancellous bone, the region of interest (ROI) was comprised of 100 slices of contoured trabecular bone above the distal growth plate (total height of 1.2 mm), and the measurements were computed at threshold settings of 1000 upper and 240 lower, with sigma of 0.4 and support of 1.0. For cortical thickness quantification, an ROI of 10 slices at a distance of 425 slices (5.1 mm) from the distal growth plate was considered for each of the femurs, using the previous settings but with a lower threshold of 275. The calculated parameters are defined as following: BV/TV is the relative volume of calcified tissue in the selected volume of interest (VOI); Tb.Th measures the thickness of the trabecular structure; Tb.N indicates the number of trabeculae; Tb.Sp indicates the trabecular separation and is inversely proportional to the trabecular thickness; and Conn.D is the connectivity density (as defined in the text); SMI is the structure model index and relates to the architecture of the structure, ranging from 0 to 3 (0 means that the structure is only plates, whereas a value of 3 means only cylindrical rods). The parameter values reported are those obtained with the direct measurement method and without model assumptions.

Statistical analysis

Difference in prevalence of bone disease between patients and controls was analyzed by the two-tailed Fisher exact test. Differences between *Rxfp2*-deficient mice and controls in the histomorphometric and μCT data were determined by unpaired two-tailed Student's *t*-test after acceptance of normal distribution with the Kolmogorov-Smirnov test. $p < 0.05$ was considered statistically significant.

RESULTS

Young men with RXFP2 gene mutations are at high risk of reduced BMD

Detailed clinical analysis surprisingly showed that 16 of 25 subjects (64.0%) with the T222P mutation in the *RXFP2* gene have reduced BMD as the sole phenotype apart from cryptorchidism at birth, despite normal plasma testosterone concentrations and the absence of other apparent causes of osteoporosis. No other biochemical or hormonal alteration was evident in these subjects, and the testicular function was normal in all patients, as evidenced by normal total and free testosterone, LH, and INSL3 concentrations (Table 1). Body mass index and body size were normal in all subjects. In particular, bone densitometry by DXA showed a femoral neck and/or lumbar spine T-score < –1 SD (osteopenia) in 10 subjects and < –2.5 SD (osteoporosis) in 6 subjects (Table 1). Careful evaluation showed that there were no differences in clinical features, history, biochemical analysis, testicular function, and hormonal levels between men with osteoporosis, osteopenia, and normal BMD. BMD was normal in 51 age-matched controls (T-score = 1.1 ± 0.2 and 1.2 ± 0.1 at the femoral neck and lumbar spine, respectively) and 20 age-matched ex-cryptorchid men without *RXFP2* and *INSL3* mutations (T-score = 1.1 ± 0.1 and 1.0 ± 0.1 at the femoral neck and lumbar spine, respectively; $p < 0.001$ versus patients with *RXFP2* mutation). Free testosterone and estradiol were in the normal range in both groups of controls: 451.6 ± 97.7 and 55.8 ± 27.2 pM, respectively, in the 51 general controls, and 425.2 ± 121.4 and 62.1 ± 37.3 pM, respectively, in the 20 ex-cryptorchid men.

Human osteoblasts possess a functional INSL3 receptor

RXFP2 mRNA expression in human bone biopsy, osteosarcoma-derived osteoblast cell line MG-63, and primary

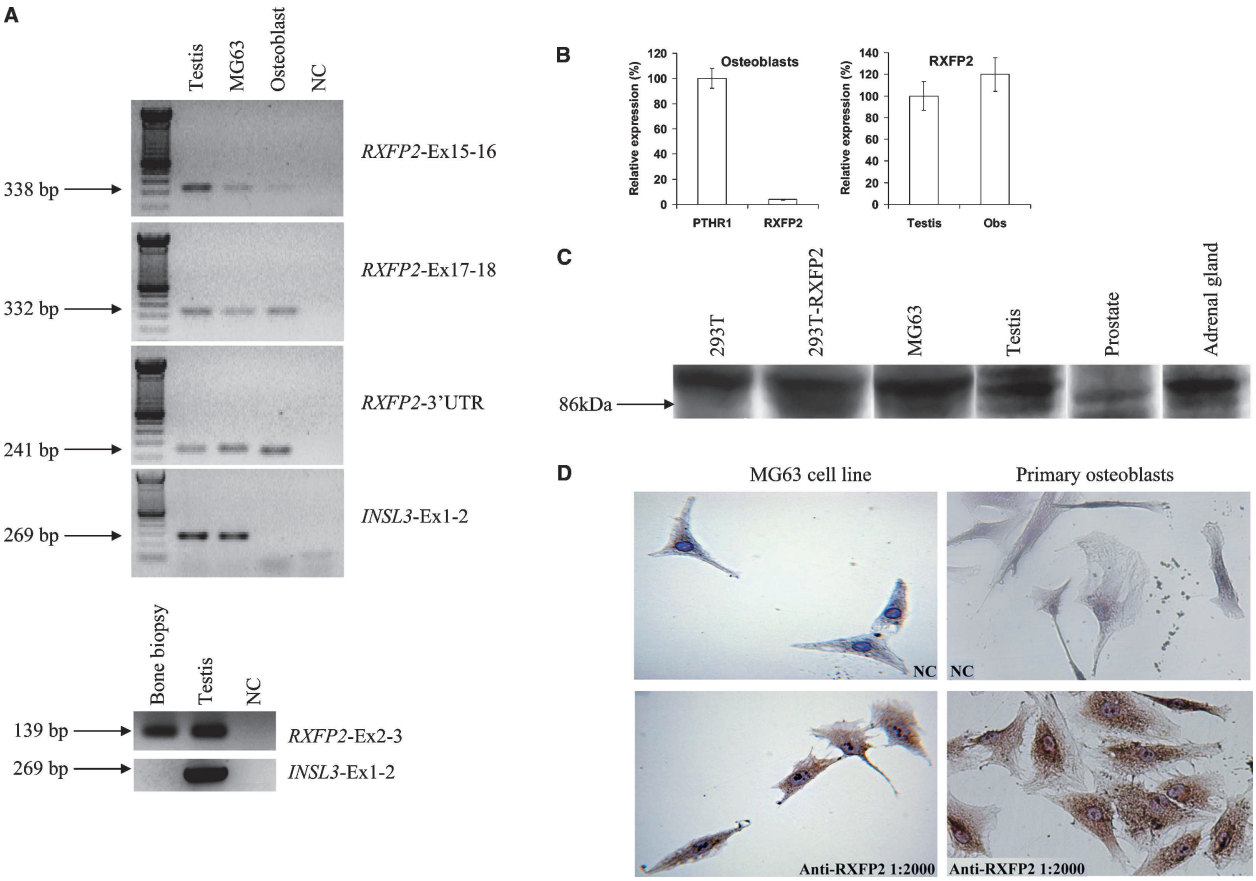

FIG. 1. Expression pattern of *RXFP2* and *INSL3* in human bone and osteoblast cells. (A) RT-PCR for *RXFP2* and *INSL3* in human testis (positive control), osteoblast cell line MG63, primary osteoblast cell culture, and human bone biopsy. On the right is indicated the set of primers used. *RXFP2* expression was evident in bone biopsy and osteoblast cells, whereas *INSL3* was present only in MG63 cells. (B) Quantitative RT-PCR analysis of *RXFP2* and *PTHR1* in human osteoblasts and *RXFP2* in human osteoblasts and testis. (C) Western blot analysis for RXFP2 expression in 293T vector cells (negative control), 293T cells transfected with *RXFP2* cDNA (positive control), MG-63 cells, testis, prostate, and adrenal gland, to confirm specificity of the RXFP2 antibody. The specific 86-kDa band was present in testis, MG-63 cells, adrenal gland, and positive control and absent in negative control and prostate. (D) Immunohistochemistry for RXFP2 in the MG-63 cell line and primary osteoblast cell culture showed the expression of RXFP2 protein in both cells. NC, negative control.

osteoblast cell culture was detected by RT-PCR and confirmed by sequencing of the amplified products (Fig. 1A). However, RT-PCR analysis showed the presence of *INSL3* mRNA only in the MG63 cell line. Quantitative RT-PCR showed that *RXFP2* expression in human osteoblasts is ~20 times lower than that of *PTHR1*, but the level of *RXFP2* expression in these cells is 20% higher than that observed in the testis (Fig. 1B).

To verify whether human osteoblasts also express the corresponding RXFP2 protein, we performed immunohistochemistry analysis. Western blotting for RXFP2 performed with the same antibody used for immunohistochemistry on total protein extracts from the cell line MG-63, 293T cells transfected with *RXFP2*, and human protein extracts from the testis and adrenal gland showed a specific band at 86 kDa (Fig. 1C), indicating the presence of the full-length receptor. This was not detected in 293T vector cells used as negative control, thus confirming the specificity of the RXFP2 antibody. Immunohistochemistry confirmed that MG63 cells and primary osteoblast cell cultures express RXFP2 protein, showing an intense cytoplasmic signal (Fig. 1D), whereas the same assay did not detect INSL3 protein expression in osteoblasts (data not shown).

We performed analysis of INSL3 signaling in the osteoblast cell line (Fig. 2). Using a FRET imaging approach, we analyzed the modification in cAMP concentrations within single living cells in vivo[24] under the stimulus of different doses of INSL3. Control experiments were performed with 293T cells transfected with *RXFP2*. Because relaxin binds RXFP2 with low affinity and potency,[9] we also used this hormone in FRET studies. Experiments were performed on cells pretreated with IBMX to block phosphodiesterase activity. Cell vitality at the end of the experiments was assessed by direct stimulation of the adenylate cyclase with forskolin. Osteoblast cell line and RXFP2-transfected 293T cells showed comparable responses to PDE inhibition with IBMX and to forskolin (data not shown). In both cell lines, human recombinant relaxin induced a small increase in intracellular cAMP levels only with the highest concentration tested (1.4 nM; Figs. 2D and 2H). Conversely, in the osteo-

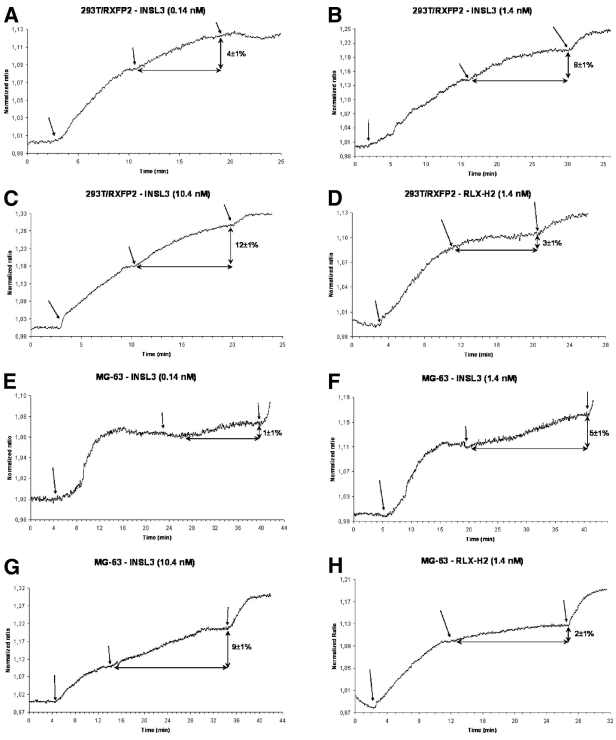

FIG. 2. Real-time imaging of cAMP in living cells by FRET imaging on 293T cells transfected with RXFP2 cDNA (positive control) (A–D) and the MG-63 osteoblast cell line (E–H), stimulated with INSL3 peptide (A–C and E–G) and recombinant human relaxin (D and H) at different doses. All the experiments were performed by blocking phosphodiesterase with IBMX (arrow on left) and controlling cell viability at the end by directly stimulating adenylate cyclase with forskolin (arrow on right). Figures show the results of one of 5–10 experiments. The percentage in intracellular cAMP increase from the plateau after IBMX is indicated as mean ± SE. INSL3 determines a dose- and time-dependent cAMP increase in MG-63 cells and 293T control cells. Minimal cAMP increase is observed after relaxin stimulus both in MG-63 cells and 293T control cells.

blast cell line, INSL3 was able to increase the cAMP production in a dose-dependent manner (Figs. 2E–2G), from 1 ± 1% at a concentration of 0.14 nM to 9 ± 1% at a concentration of 10.4 nM. The magnitude of cAMP increase in osteoblast cells after INSL3 stimulation was comparable to that observed in control 293T cells transfected with RXFP2 cDNA (Figs. 2A–2C).

The culture of human primary osteoblasts at serial INSL3 concentrations, from 0.01 to 10 nM, induced a significant and dose-dependent increase in proliferation (Fig. 3), further supporting a role of INSL3 on osteoblast function.

Taken together, these experimental and clinical data in humans suggest for the first time an endocrine role for INSL3 hormone in bone physiology and link *RXFP2* gene mutations with reduced BMD and osteoporosis in men.

Rxfp2-deficient mice show reduced bone mass

To support our clinical and experimental findings in humans, we looked for an animal model with perturbed INSL3/RXFP2 signaling. We first showed *Rxfp2* expression

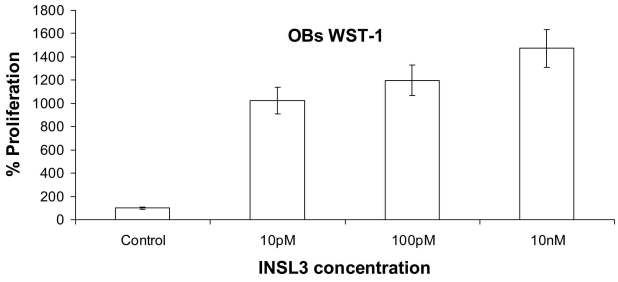

FIG. 3. Proliferation assay of human osteoblasts measured by WST-1 and absorbance at 440 nm in the presence of different doses of INSL3. Data are expressed as percentage with respect to the negative control (not stimulated), and the values are the mean ± SD of the mean of three independent experiments performed in triplicate.

in mouse primary osteoblast cells by RT-PCR, confirming our data from the human samples (Fig. 4A), and then we analyzed male mice lacking *Rxfp2*.[10]

μCT (Figs. 4B and 4C; Table 3) was performed at both the cortical bone at the midshaft and the trabecular bone at the distal end of the femur. Whereas no differences were noted in the cortical bone between the two genotypes, the quantification of the trabecular bone in the distal femur showed significantly decreased bone volume (BV/TV; Fig. 4B; Table 3) and trabecular number (Tb.N) and increased trabecular separation (Tb.Sp) in the *Rxfp2*$^{-/-}$ compared with the WT mice (Table 3). Although these differences were statistical significant, trabecular thickness was not affected. The structure model index (SMI) suggested a trabecular bone with increased prevalence of cylindrical rods versus plates in the *Rxfp2*$^{-/-}$ mice (Table 3), which is typical of a weaker bone.

Histomorphometric analysis[27,28] of the lumbar spine (L_3–L_4) showed a statistical significant reduction in bone volume/tissue volume (BV/TV) in *Rxfp2*$^{-/-}$ compared with WT mice ($p = 0.027$). Trabecular thickness (Tb.Th), however, was not significantly affected (data not shown). The osteoblast surface (Ob.S/BS), which is directly correlated with the number of osteoblasts, is reduced in *Rxfp2*$^{-/-}$ mice compared with WT mice, but this difference was not statistically significant (Fig. 5B). The number of osteoclasts (Oc./B.Pm) was not different between the two genotypes; however, the osteoclast surface (Oc.S/BS) was statistically reduced in *Rxfp2*$^{-/-}$ compared with WT mice ($p < 0.01$; Fig. 5A). Analysis of dynamic parameters of bone formation showed that, whereas the MAR was not changed, the mineralizing surface (MS/BS) and the bone formation rate (BFR/BS) were statistically decreased in *Rxfp2*$^{-/-}$ compared with WT mice ($p < 0.01$; Fig. 5A).

Taken together, these data suggest that *Rxfp2*-deficient male mice are osteopenic and have a functional osteoblast impairment, and their phenotype resembles that of humans with *RXFP2* mutations.

DISCUSSION

This study suggests for the first time a role for INSL3/RXFP2 signaling in bone metabolism and shows that young

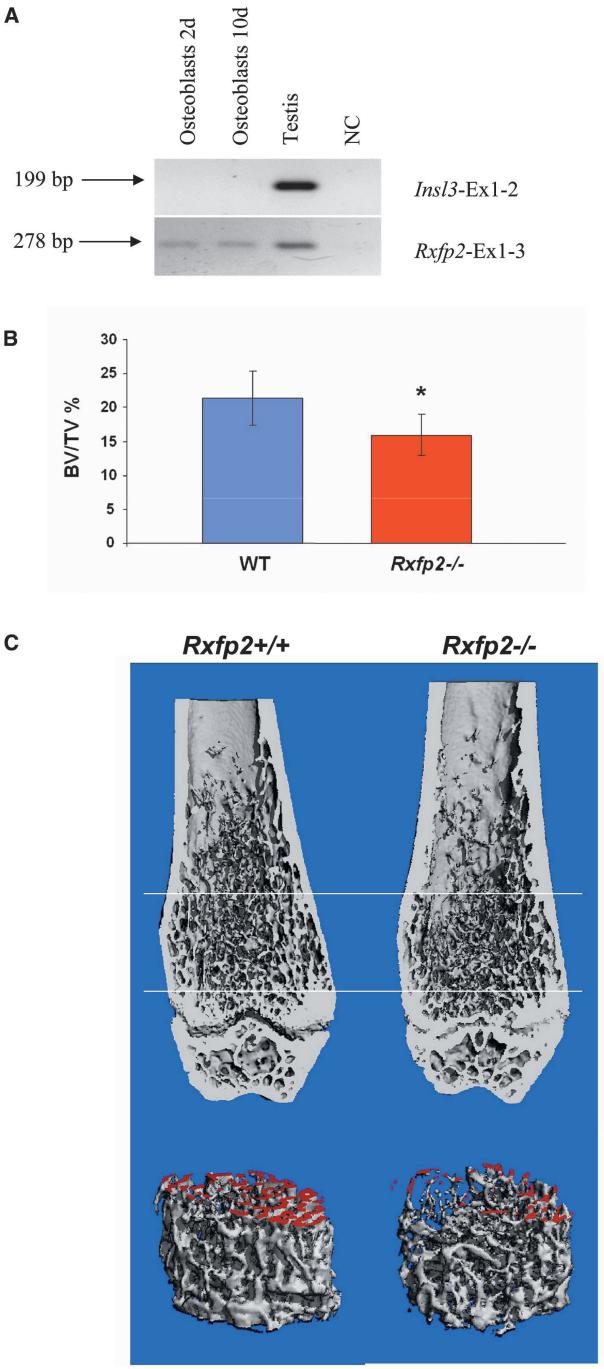

FIG. 4. Expression of *Rxfp2* and *Insl3* in mouse osteoblasts and bone analysis of *Rxfp2*-deficient mouse. (A) Expression of *Rxfp2* is observed in testis (positive control) and osteoblasts after 2 and 10 days of culture, whereas no *Insl3* expression was observed in these cells. (B) Bone volume/tissue volume (BV/TV), expressed as percentage, calculated from μCT of the distal femur of 8-wk-old $Rxfp2^{-/-}$ and $Rxfp2^{+/+}$ male mice. BV/TV values are (mean ± SD) as follows: 21.4 ± 3.9 for WT and 15.9 ± 3.0 for $Rxfp2^{-/-}$ ($p < 0.01$). (C) μCT 3D reconstruction of distal femurs from *Rxfp2*-mutant and WT mice. (Top) A representative medial coronal view of a 3D reconstructed distal femur shows decreased trabecular bone in the $Rxfp2^{-/-}$ vs. the WT control femur. (Bottom) μCT 3D reconstruction of trabecular bone delimited by the two cross planes (white bars) in the top part (distance is 1.2 mm). Trabecular surfaces generated by the cutting of the proximal cross plane are artificially colored in red.

TABLE 3. μCT QUANTIFICATION OF DISTAL FEMURS OF WT AND $RXFP2^{-/-}$ MICE

	WT	$Rxfp2^{-/-}$	
BV/TV (%)	21.419 ± 3.980	15.976 ± 3.050	$p = 0.014$*
Tb.Th (mm)	0.043 ± 0.003	0.039 ± 0.004	$p = 0.056$
Tb.N (1/mm)	6.978 ± 0.620	6.198 ± 0.448	$p = 0.019$*
Tb.Sp (mm)	0.142 ± 0.015	0.163 ± 0.013	$p = 0.016$*
Conn.D ($1/mm^3$)	451.534 ± 61.670	366.623 ± 86.8000	$p = 0.056$
SMI	1.686 ± 0.279	2.079 ± 0.274	$p = 0.021$*
Ct.Th (mm)	0.196 ± 0.010	0.199 ± 0.018	$p = 0.707$

Values are mean ± SD of $n = 7$.
* Statistical significance.
BV/TV, volume of calcified tissue in the selected volume of interest; Tb.Th, thickness of the trabecular structure; Tb.N, number of trabeculae; Tb.Sp, trabecular separation; Conn.D, 3D connectivity index; SMI, structure model index; Ct.Th, cortical thickness.

men with *RXFP2* gene mutations are at increased risk of osteoporosis. We found that 16 of 25 (64%) young men with *RXFP2* mutations had significantly reduced BMD, represented by osteopenia or osteoporosis. No other apparent cause of osteoporosis was evident in these subjects, whose testosterone level and gonadal function were normal. Expression analyses showed the presence of RXFP2 in human and mouse osteoblasts. Stimulation of these cells with INSL3 produced a dose- and time-dependent increase in cAMP, confirming the functionality of the RXFP2/INSL3 receptor–ligand complex and a dose-dependent increase in osteoblast proliferation. Consistent with the human phenotype, bone analyses of $Rxfp2^{-/-}$ mice showed osteopenia with decreased bone mass and altered trabecular organization typical of a weaker bone. In particular, whereas the osteoblast surface is normal in $Rxfp2^{-/-}$ mice, the mineralizing surface over the bone surface is clearly reduced and hence caused a decrease in BFR. The number of osteoclasts is normal in these mice, but the osteoclast surface is reduced, suggesting a less matured/differentiated population of osteoclasts. This suggests that the low bone mass phenotype in the $Rxfp2^{-/-}$ mice is not caused by a hyper-resorptive state but by functional alterations in the osteoblast compartment causing little bone formation, little mineralizing surface, and ultimately, a negative balance between bone formation and bone resorption.

We did not find expression of INSL3 in bones, and thus the effect of INSL3 seems to be endocrine rather than autocrine/paracrine. The major source of INSL3 is the Leydig cells of the testis and significant circulating levels of this hormone are found only in men, the concentrations in women being very low.[2] In association with the other testicular hormone testosterone, INSL3 seems therefore to represent a male-specific factor regulating BMD. Because no other abnormalities were detected in men with RXFP2 mutations, our findings suggest that the main INSL3 function in adult men might be related to bone development and physiology. Reduced INSL3 plasma levels are observed only in subjects with impairment of Leydig cell differentiation and function, such as hypogonadal men.[2] In these cases and other clinical situations where testicular function is affected, testosterone concentration is often reduced, and

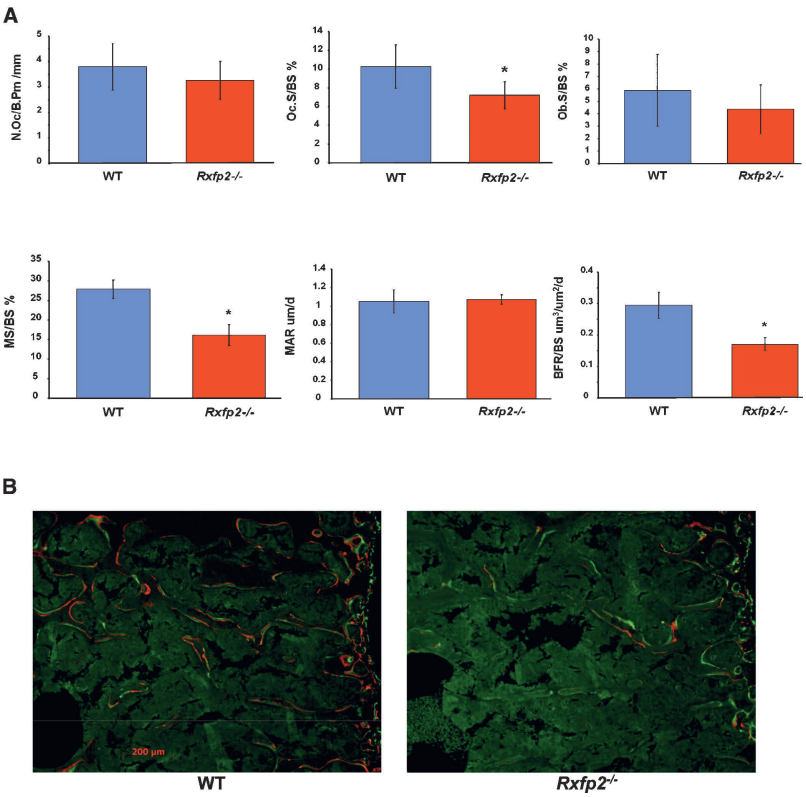

FIG. 5. Static and dynamic (bone formation indices) histomorphometric analysis of lumbar spine of WT and *Rxfp2*$^{-/-}$ mice. (A) Histograms showing the number of osteoclasts per bone perimeter (N.Oc/B.Pm, mm), the osteoclast surface (Oc.S/BS, %), the osteoblast surface (Ob.S/BS, %), the mineralizing surface (MS/BS, %), the mineral apposition rate (MAR, µm/d), and the bone formation rate (µm^3/µm^2/d). *$p < 0.01$. (B) Representative double label images showing the incorporation of the two fluorescent dyes (Alizarin-3-methylmino-diacetic acid and calcein), injected 4 days apart, into the mineralizing osteoid and showing the dramatic difference in MS/BS.

therefore, it is difficult to discern the contribution of low INSL3 levels on bone pathology. On the contrary, all human patients with *RXFP2* mutations and mutant mouse males[4] had normal serum testosterone levels and testicular function, including normal INSL3 levels, suggesting that INSL3 signal deficiency in bones can not be compensated by male steroid hormones.

The findings of this study showed that disruption of the INSL3 hormonal system, as observed in humans and mice with mutations in *RXFP2* gene, might have a pathogenic role in bone loss, providing evidence for a novel genetic cause of human osteoporosis. Bone loss in men with reduced INSL3 activity is most likely progressive over time and influenced by other factors, and this might explain why not all young men with *RXFP2* mutations observed in this study have osteoporosis. The etiology of male osteoporosis, particularly in young and middle-aged men, is often unknown (primary or idiopathic osteoporosis), although probably related to osteoblast dysfunction. Genetic susceptibility has been evoked, but clear genetic etiology has not been identified. Importantly, *RXFP2* maps to chromosome 13q13, and it is worthy to note that whole genome scans have linked several regions on chromosome 13q to osteoporosis,[29–32] and in particular, the regions 13q12 and 13q14 have been associated with reduced BMD in men and not in women.[30,32] With the identification of osteoblasts as INSL3-responsive cells and the association between mutations in the *INSL3* receptor gene and decreased BMD, our study opens new perspectives not only in diagnostic male osteoporosis but also in age-associated osteoporosis and familial osteoporosis and provides a starting point for potential development of new therapeutic approaches to these conditions.

ACKNOWLEDGMENTS

We thank Francesco Di Virgilio for helpful advice and Massimo Menegazzo, Luca De Toni, Massimiliano Bicego, Giulietta Di Benedetto, and Anne Truong for technical assistance. The financial support of the University of Padova (to AF), NIH Grants R01 HD37067 (to AIA) and AR051459 (to RM), the Osteogenesis Imperfecta Foundation and The Bone Disease Program of Texas (to RM), Telethon Foundation Grants TCP00089 and GGP05113 (to MZ), HFSPO Grant RGP0001/2005-C (to MZ), Compagnia di San Paolo (to MZ), and Italian Cystic Fibrosis Research Foundation (to MZ) is gratefully acknowledged. The Center for Research in Reproduction Ligand Assay and Analysis Core at the University of Virginia is supported by NICHD Grant U54 HD28934. Funders had no role in the design and conduct of the study, in the collection, analysis, and interpretation of the data, and in the preparation, review, or approval of the manuscript.

REFERENCES

1. Adham IM, Burkhardt E, Benahmed M, Engel W 1993 Cloning of a cDNA for a novel insulin-like peptide of the testicular Leydig cells. J Biol Chem **268:**26668–26672.
2. Foresta C, Bettella A, Vinanzi C, Dabrilli P, Meriggiola MC,

Garolla A, Ferlin A 2004 Insulin like factor 3: A novel circulating hormone of testis origin in humans. J Clin Endocrinol Metab **89:**5952–5958.
3. Ferlin A, Arredi B, Zuccarello D, Garolla A, Selice R, Foresta C 2006 Paracrine and endocrine roles of insulin-like factor 3. J Endocrinol Invest **29:**657–664.
4. Overbeek PA, Gorlov IP, Sutherland RW, Houston JB, Harrison WR, Boettger-Tong HL, Bishop CE, Agoulnik AI 2001 A transgenic insertion causing cryptorchidism in mice. Genesis **30:**26–35.
5. Hsu SY, Nakabayashi K, Nishi S, Kumagai J, Kudo M, Sherwood OD, Hsueh AJ 2002 Activation of orphan receptors by the hormone relaxin. Science **295:**671–674.
6. Kumagai J, Hsu SY, Matsumi H, Roh JS, Fu P, Wade JD, Bathgate RA, Hsueh AJ 2002 INSL3/Leydig insulin-like peptide activates the LGR8 receptor important in testis descent. J Biol Chem **277:**31283–31286.
7. Bogatcheva NV, Truong A, Feng S, Engel W, Adham IM, Agoulnik AI 2003 GREAT/LGR8 is the only receptor for insulin-like 3 peptide. Mol Endocrinol **17:**2639–2646.
8. Bathgate RA, Ivell R, Sanborn BM, Sherwood OD, Summers RJ 2006 International Union of Pharmacology LVII: Recommendations for the nomenclature of receptors for relaxin family peptides. Pharmacol Rev **58:**7–31.
9. Halls ML, van der Westhuizen ET, Bathgate RA, Summers RJ 2007 Relaxin Family Peptide Receptors - former orphans reunite with their parent ligands to activate multiple signalling pathways. Br J Pharmacol **150:**677–691.
10. Gorlov IP, Kamat A, Bogatcheva NV, Jones E, Lamb DJ, Truong A, Bishop CE, McElreavey K, Agoulnik AI 2002 Mutations of the GREAT gene cause cryptorchidism. Hum Mol Genet **11:**2309–2318.
11. Nef S, Parada LF 1999 Cryptorchidism in mice mutant for Insl3. Nat Genet **22:**295–299.
12. Zimmermann S, Steding G, Emmen JM, Brinkmann AO, Nayernia K, Holstein AF, Engel W, Adham IM 1999 Targeted disruption of the Insl3 gene causes bilateral cryptorchidism. Mol Endocrinol **13:**681–691.
13. Ferlin A, Simonato M, Bartoloni L, Rizzo G, Bettella A, Dottorini T, Dalla piccola B, Foresta C 2003 The INSL3-LGR8/GREAT ligand-receptor pair in human cryptorchidism. J Clin Endocrinol Metab **88:**4273–4279.
14. Ferlin A, Bogatcheva NV, Gianesello L, Pepe A, Vinanzi C, Agoulnik AI, Foresta C 2006 Insulin-like factor 3 gene mutations in testicular dysgenesis syndrome: Clinical and functional characterization. Mol Hum Reprod **12:**401–406.
15. Bogatcheva NV, Ferlin A, Feng S, Truong A, Gianesello L, Foresta C, Agoulni KAI 2007 T222P mutation of the insulin-like 3 hormone receptor LGR8 is associated with testicular maldescent and hinders receptor expression on the cell surface membrane. Am J Physiol Endocrinol Metab **292:**E138–E144.
16. Bay K, Matthiesson KL, McLachlan RI, Andersson AM 2006 The effects of gonadotropin suppression and selective replacement on insulin-like factor 3 secretion in normal adult men. J Clin Endocrinol Metab **91:**1108–1111.
17. Sadeghian H, Anand-Ivell R, Balvers M, Relan V, Ivell R 2005 Constitutive regulation of the Insl3 gene in rat Leydig cells. Mol Cell Endocrinol **241:**10–20.
18. Ferlin A, Garolla A, Rigon F, Rasi Caldogno L, Lenzi A, Foresta C 2006 Changes in serum Insulin-like factor 3 (INSL3) during normal male puberty. J Clin Endocrinol Metab **91:**3426–3431.
19. Kawamura K, Kumagai J, Sudo S, Chun SY, Pisarska M, Morita H, Toppari J, Fu P, Wade JD, Bathgate RA, Hsueh AJ 2004 Paracrine regulation of mammalian oocyte maturation and male germ cell survival. Proc Natl Acad Sci USA **101:**7323–7328.
20. Anand-Ivell RJ, Relan V, Balvers M, Coiffec-Dorval I, Fritsch M, Bathgate RA, Ivell R 2006 Expression of the insulin-like peptide 3 (INSL3) hormone-receptor (LGR8) system in the testis. Biol Reprod **74:**945–953.
21. Hombach-Klonisch S, Hoang-Vu C, Kehlen A, Hinze R, Holzhausen HJ, Weber E, Fischer B, Dralle H, Klonisch T 2003 INSL-3 is expressed in human hyperplastic and neoplastic thyrocytes. Int J Oncol **22:**993–1001.
22. Hombach-Klonisch S, Buchmann J, Sarun S, Fischer B, Klonisch T 2000 Relaxin-like factor (RLF) is differentially expressed in the normal and neoplastic human mammary gland. Cancer **89:**2161–2168.
23. Vermeulen A, Verdonck L, Kaufman JM 1999 A critical evaluation of simple methods for the estimation of free testosterone in serum. J Clin Endocrinol Metab **84:**3666–3672.
24. Zaccolo M, De Giorgi F, Cho CY, Feng L, Knapp T, Negulescu PA, Taylor SS, Tsien RY, Pozzan T 2000 A genetically encoded, fluorescent indicator for cyclic AMP in living cells. Nat Cell Biol **2:**25–29.
25. Ponsioen B, Zhao J, Riedl J, Zwartkruis F, van der Krogt G, Zaccolo M, Moolenaar WH, Bos JL, Jalink K 2004 Detecting cAMP-induced Epac activation by fluorescence resonance energy transfer: Epac as a novel cAMP indicator. EMBO Rep **5:**1176–1180.
26. Zaccolo M, Pozzan T 2002 Discrete microdomains with high concentration of cAMP in stimulated rat neonatal cardiac myocytes. Science **295:**1711–1715.
27. Parfitt AM, Drezner MK, Glorieux FH, Kanis JA, Malluche H, Meunier PJ, Ott SM, Recker RR 1987 Bone histomorphometry: Standardization of nomenclature, symbols, and units. Report of the ASBMR Histomorphometry Nomenclature Committee. J Bone Miner Res **2:**595–610.
28. Morello R, Bertin TK, Chen Y, Hicks J, Tonachini L, Monticone M, Castagnola P, Rauch F, Glorieux FH, Vranka J, Bächinger HP, Pace JM, Schwarze U, Byers PH, Weis M, Fernandes RJ, Eyre DR, Yao Z, Boyce BF, Lee B 2006 CRTAP is required for prolyl 3- hydroxylation and mutations cause recessive osteogenesis imperfecta. Cell **127:**291–304.
29. Niu T, Chen C, Cordell H, Yang J, Wang B, Wang Z, Fang Z, Schork NJ, Rosen CJ, Xu X 1999 A genome-wide scan for loci linked to forearm bone mineral density. Hum Genet **104:**226–233.
30. Kammerer CM, Schneider JL, Cole SA, Hixson JE, Samollow PB, O'Connell JR, Perez R, Dyer TD, Almasy L, Blangero J, Bauer RL, Mitchell BD 2003 Quantitative trait loci on chromosomes 2p, 4p, and 13q influence bone mineral density of the forearm and hip in Mexican Americans. J Bone Miner Res **18:**2245–2252.
31. Deng HW, Xu FH, Huang QY, Shen H, Deng H, Conway T, Liu YJ, Liu YZ, Li JL, Zhang HT, Davies KM, Recker RR 2002 A whole-genome linkage scan suggests several genomic regions potentially containing quantitative trait Loci for osteoporosis. J Clin Endocrinol Metab **87:**5151–5159.
32. Tang ZH, Xiao P, Lei SF, Deng FY, Zhao LJ, Deng HY, Tan LJ, Shen H, Xiong DH, Recker RR, Deng HW 2007 A bivariate whole-genome linkage scan suggests several shared genomic regions for obesity and osteoporosis. J Clin Endocrinol Metab **92:**2751–2757.

Address reprint requests to:
Carlo Foresta, MD
University of Padova
Department of Histology, Microbiology, and Medical Biotechnologies
Centre for Male Gamete Cryopreservation
Via Gabelli 63
35121 Padova, Italy
E-mail: carlo.foresta@unipd.it

Received in original form September 5, 2007; revised form January 29, 2008; accepted january 29, 2008.